

Dynamic Mode AFM Measurement of CMUT Diaphragm Deflection Profile

Sazzadur Chowdhury

Department of Electrical and Computer Engineering

University of Windsor

Windsor, ON, N9B 3P4, Canada

e-mail: sazzadur@uwindsor.ca

Abstract—Atomic Force Microscopy (AFM) measurement results of the deflection shape and ISO 25178 roughness parameters of the diaphragm of an adhesive wafer bonded Silicon-on-Insulator (SOI) based Capacitive Micromachined Ultrasonic Transducer (CMUT) has been presented. The AFM measurements were carried out using the dynamic mode operation of an atomic force microscope to achieve higher resolution. The measurement results were used to construct the 3D deflection shape of the CMUT diaphragm with actual height parameters. The measured deflection shape of the CMUT diaphragm can be used to determine the stiffness, residual stress, and other physical parameters in a CMUT diaphragm to facilitate more accurate calibration and CMUT sensitivity.

Keywords—CMUT; SOI; AFM; Dynamic mode; Residual stress.

I. INTRODUCTION

Capacitive Micromachined Ultrasonic Transducers (CMUT) are advantageous over the piezoelectric ultrasonic transducers as they offer superior sensitivity, better temporal and axial resolution, higher fractional bandwidth, and higher energy transduction efficiency [1]. CMUTs also offer lower mechanical impedance, lower self-heating, lower dielectric loss, lower internal loss, and better thermal dissipation than their piezoelectric counterparts [1]-[4]. All of these positive features of CMUTs translate into better image quality as has been experimentally verified in [5]-[7]. Additionally, unlike the piezoelectric transducers, the CMUTs can be batch fabricated with sub-micrometer resolution using CMOS compatible highly matured conventional microelectronic fabrication techniques to reduce per unit production cost [7].

The CMUTs rely on electrostatic or acoustic vibration of a thin diaphragm which is separated from a fixed backplate by a thin airgap or vacuum space to generate ultrasound in a surrounding medium (transmit mode) or to generate an electrical signal corresponding to an incident ultrasound wave on the diaphragm (receive mode) [1]-[3]. As the CMUTs rely on the vibration of a diaphragm to transmit or receive ultrasound, accurate measurement of the deflection profile (shape) of the diaphragm and surface roughness is crucial for proper characterization of transducer operation [8].

The deflection profile of a diaphragm depends on the stiffness of the diaphragm that in turn depends on the shape of the diaphragm, support conditions, homogeneity of the diaphragm material, residual stress, Poisson ratio, diaphragm

thickness uniformity and the shape of the cavity. The CMUT cavity is either a sealed vacuum entity or filled with atmospheric air if the diaphragm has perforations.

A CMUT diaphragm experiences different types of stresses, such as tensile or compressive residual stress due to the fabrication process, stress due to atmospheric pressure indentation (vacuum cavity), and stress due to the expansion of the trapped residual gas in the sealed cavity during fabrication [9]. Fabrication process induced imperfections may also contribute to cavity shape alternations, diaphragm thickness variation, and the quality of the diaphragm. Consequently, such structural imperfections affect the electrostatic pressure generation during transmit operation or capacitive readout during ultrasound reception. A measurement of the diaphragm deflection profile and surface roughness can be used to determine proper balance of laminate thickness of different materials used to fabricate the diaphragm, improve thickness uniformity of the diaphragm, material properties adjustments by modifying fabrication process parameters and steps to achieve optimized residual stress. All of these will contribute to superior yield, superior array operation, and better imaging resolution.

Optical profilometry is one of the widely used techniques for surface characterization in microfabrication applications. White Light Interferometry (WLI), Confocal Laser Scanning (CLS) microscopy, and Confocal Grid Structured Illumination (CGSI) microscopy are commonly used techniques to characterize thinfilm thickness, reflectivity, and height measurement. Stylus based contact profilometry techniques are also used but that needs additional fabrication steps to prepare the sample and imposes risk of device damage. Possible uses of different optical profilometry techniques for CMUT characterization are available in [9].

In this context, this paper presents initial results of the dynamic (tapping) mode AFM characterization of the deflection profile of a CMUT diaphragm [10][11]. The measurements were carried out using a FlexAFM™ with C3000 controller from Nanosurf™ [10]. Relative advantages and disadvantages of AFM as compared to optical systems have also been discussed in the context of CMUT diaphragm deflection profile characterization.

The rest of the paper has been organized in the following way: In Section II, major specifications of the measured CMUT sample are given. Section III provides a brief theoretical description of the dynamic mode AFM, Section IV provides AFM measurement set up and data processing and finally Section V makes the concluding remarks.

II. CMUT SPECIFICATIONS

A cross section of the measured CMUT sample is shown in Figure 1 and the device specifications are provided in Table I. The CMUT was fabricated using an adhesive wafer bonding technique using BCB as the dielectric spacer and the device layer of an SOI wafer was used to realize the CMUT diaphragm [12].

Figure 2 shows a Scanning Electron Microscope (SEM) image of one of the diced CMUT cell array. The array was fabricated for an automotive collision avoidance application. Detailed description of the fabrication process is available in [12].

TABLE I. CMUT CELL SPECIFICATIONS

Parameter	Value	Unit
Diaphragm laminate thickness	800	nm
Gold layer thickness	100	nm
Silicon device layer thickness	700	nm
Cavity thickness	1	μm
Cavity width	28	μm
Sidewall width	10	μm
Bottom wafer thickness	500	μm

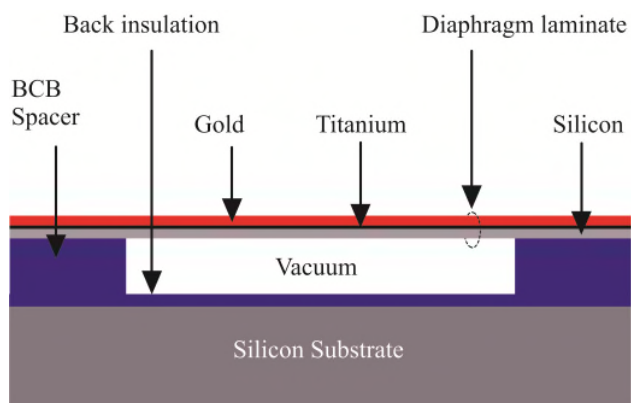


Figure 1. Cross-section of the measured CMUT cell.

The array has 40 x 40 CMUT cells with specifications as listed in Table I in a footprint area of 1870 x 1870 μm².

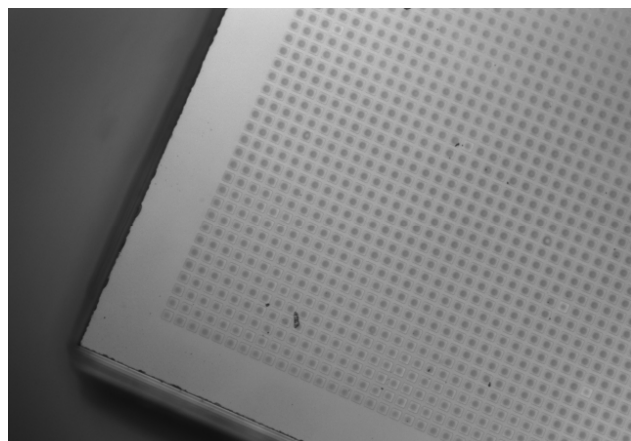


Figure 2. SEM image of a singulated CMUT die.

III. AFM DYNAMIC MODE OPERATION

An AFM technique creates a 3D topography of the sample's surface using a cantilever probe with a sharp tip as the probe or the sample is scanned in x-y plane [10][11]. As an AFM provides the vertical height data directly from measurements, the technique is very different from an optical imaging microscope, which measures a two-dimensional projection of a sample's surface [13].

Despite the advantages of the optical systems as summarized in [13], as a two-dimensional image from an optical system does not have any height information in it, such images must infer the height information from the image or rotate the sample to see feature heights [13]. The AFM also provides various types of surface measurements and can generate images at atomic resolution with angstrom scale resolution height information for both conducting and insulating surfaces with minimum sample preparation [14]. In [15], it has been mentioned that the spatial and "Z" resolution of the AFM is much better than that could be obtained by an optical profilometer whatever optical system is used. In [15], it has also been mentioned that the AFM images are more faithful to nanoscale surface topographic variations compared to optical profilometers. Furthermore, an AFM measuring system is free of any errors related to optical focusing, depth of field adjustment, or sample illumination angles. Consequently, an AFM allows one to measure surface topography with unprecedented resolution and accuracy [16]. As the capacitance change during the CMUT diaphragm vibration is very small (attofarad to femtofarad range) corresponding to picometer range deflection of the CMUT diaphragm, precision measurement of the diaphragm deflection profile is crucial for proper characterization of CMUT operation to improve imaging resolution.

For the current research work, the AFM measurements were done using a FlexAFM™ from Nanosurf™ operating in dynamic mode. The dynamic mode was chosen over the static mode due to the fact that the static mode AFM does not achieve atomic resolution due to the mesoscopic properties of the tip, which induces a contact zone dispersed over many atoms as opposed to a single atom [11]. Additionally, the dynamic mode offers the following advantages: (1) gentle interaction of the probe tip with the surface during tapping to preserve the sharpness of the tip to improve accuracy, (2) minimized torsional forces between the probe and the sample, and (3) by using the cantilever's oscillation amplitude as the feedback parameter, the user is able to fine-tune the interaction between probe and sample between different regimes- such as attractive and repulsive ones- to control the tip-surface distance on an atomic scale [10].

The dynamic mode operation of an AFM is illustrated conceptually in Figure 3. During operation, the cantilever is forced to vibrate at its resonance frequency using a piezo element. As the oscillating cantilever is brought closer to the sample surface, it experiences a repulsive force that increases the resonance frequency of the cantilever and its vibration amplitude decreases [10]. The vibration amplitude of the

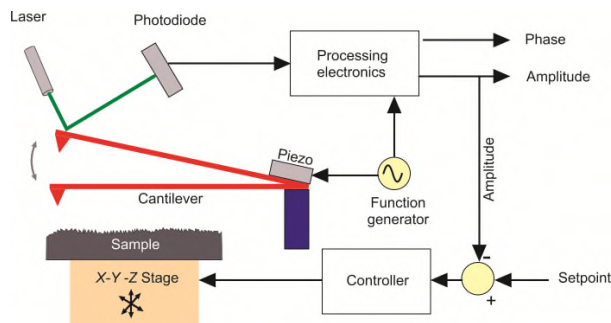


Figure 3. AFM dynamic mode operation.

cantilever is detected using a laser and photodiode based detection system as shown in Figure 3.

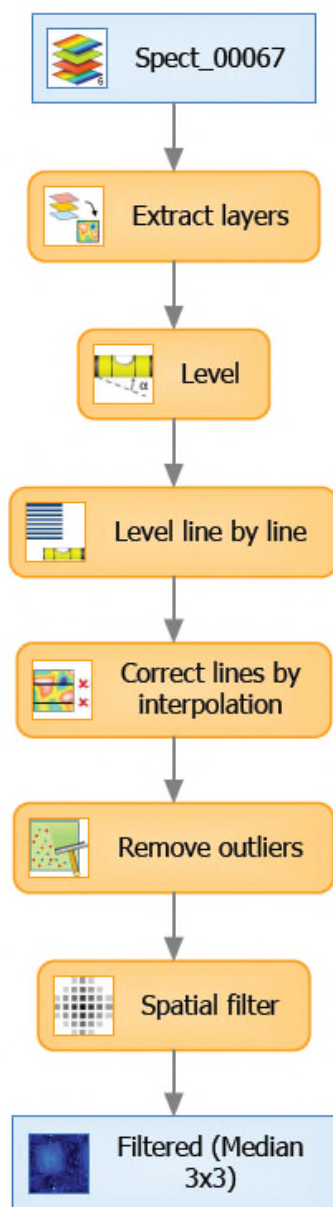


Figure 4. FlexAFM Spect-0067 data processing steps.

The measured laser beam deflection or cantilever vibration amplitude is then used as an input for a feedback loop that keeps the tip-sample interaction constant by changing the tip height. The output of this feedback loop thus corresponds to the local sample height. This amplitude reduction is a direct measure of the feature height on the sample surface that is mapped in a 2-D x - y plane [10][11].

IV. THE AFM MEASUREMENT SET UP FOR CMUT

The AFM measurements of the CMUT sample were done using FlexAFM™ with C3000 controller from Nanosurf™ operating in dynamic mode with active vibration isolation and acoustic isolation.

An ACLA™ cantilever with nominal spring constant of 58 N/m was used to collect the data. The ACLA™ probes are silicon probes with long cantilevers used for tapping mode and other applications that allow for larger laser clearance, and have aluminum coating on the reflex side to increase laser signal quality. Detailed measurement setup instructions are available in [17].

Once the AFM measurement was done, the height data was processed following standard AFM data processing steps as shown in Figure 4. The generated pseudo-color view of the surface is shown in Figure 5. The Gwyddion™ [18] AFM data processing software has been used next to generate a 3-D height image of the surface as shown in Figure 6. The statistical roughness parameters following ISO 25178 have been extracted using Gwyddion™ and provided in Table II.

As the AFM data are usually collected as line scans along the x axis that are concatenated together to form a two-dimensional image, the scanning speed in the x direction is considerably higher than the scanning speed in the y direction. As a result, the x profiles are less affected by low frequency noise and thermal drift of the sample as compared to the y profile [18].

Consequently, standardized one dimensional roughness parameters are considered more accurate [18]. Accordingly, the one dimensional roughness parameters for a scan line centered approximately at the middle of the CMUT diaphragm along the y -axis direction as shown in Figure 7 was extracted using Gwyddion™ and are plotted in Figure 8.

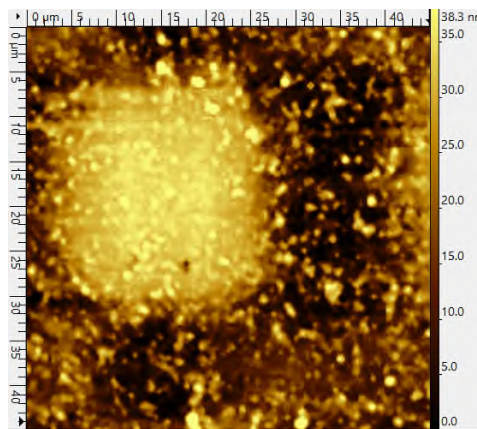


Figure 5. Pseudo-color image of the sample.

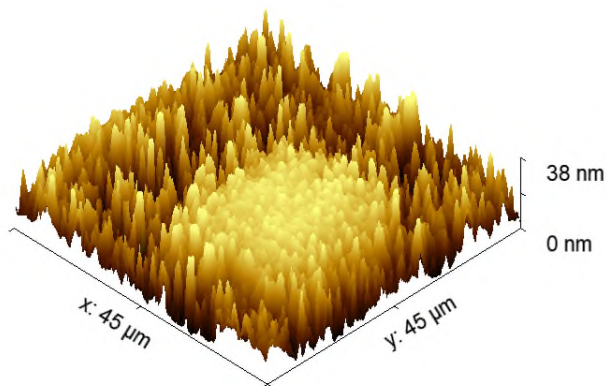


Figure 6. 3D height image of the sample.

TABLE II. STATISTICAL ROUGHNESS PARAMETERS

Parameter	Value	Unit
RMS roughness, S_q	10.50	nm
Mean-square roughness, S_a	9.08	nm
Skew (S_{sk})	0.06925	
Excess kurtosis	-1.185	
Maximum peak height, S_p	19.24	nm
Maximum pit depth, S_v	19.01	nm
Maximum height, S_z	38.25	nm
Projected area:	2025	μm^2
Surface area	2026	μm^2
Volume	38.50	μm^3

Corresponding texture and waviness data are also shown. Detailed roughness parameters along this scan line are provided in Table III. The waviness average along this particular scanning line as determined from Gwyddion™ is 8.77 nm with a cut-off wavelength of 7.69 μm . The same measurement was carried out along a y-axis scanning line as shown in Figure 9 and the corresponding texture, roughness, and waviness parameters are shown in Figure 10. Finally, the waviness parameters are plotted for an arbitrary diagonal direction as shown in Figure 11 and the corresponding waviness profile is shown in Figure 12.

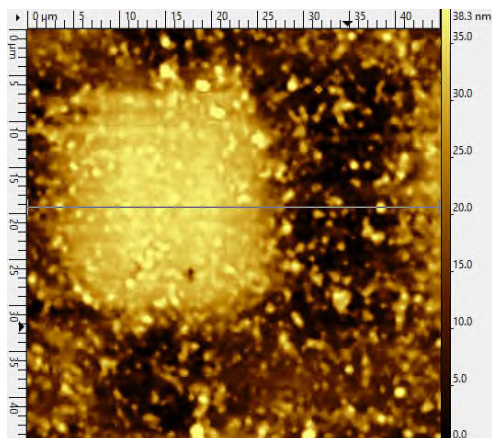


Figure 7. Scan line to determine standardized roughness parameters along the x-axis direction.

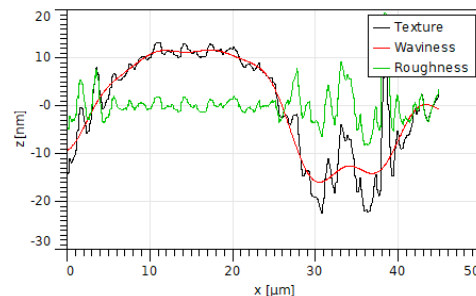


Figure 8. Roughness, texture, and waviness profile along an x-directional scan line as shown in Figure 7.

TABLE III. ONE DIMENSIONLA ROUGHNESS PARAMETERS

Parameter	Value	Unit
Cut-off	7.69	μm
Roughness average (R_a)	3.09	nm
Root mean square roughness (R_q)	4.87	nm
Maximum height of the roughness (R_t)	34.58	nm
Maximum roughness valley depth (R_v)	10.67	nm
Maximum roughness peak height (R_p)	23.91	nm
Average maximum height of the roughness (R_m)	17.92	nm
Average maximum roughness valley depth (R_{vm})	6.97	nm
Average maximum roughness peak height (R_{pm})	10.95	nm
Average third highest peak to third lowest valley height (R_{3v})	20.34	nm
Average third highest peak to third lowest valley height (R_{3z} ISO)	14.38	nm
Average maximum height of the profile (R_z)	20.83	nm
Average maximum height of the roughness (R_z ISO)	17.92	nm
Maximum peak to valley roughness ($R_y = R_{max}$)	34.58	nm
Skewness (R_{sk})	1.87	
Kurtosis (R_{ku})	10.46	
Waviness average (W_a)	8.77	nm
Root mean square waviness (W_q)	10.16	nm

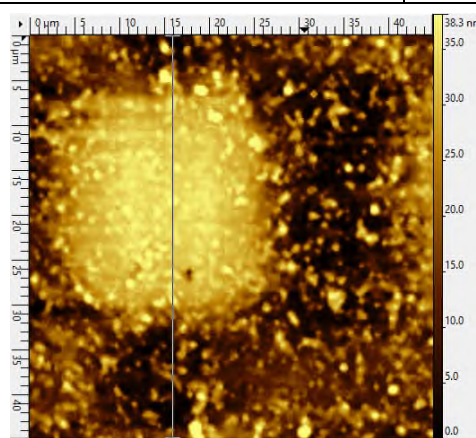


Figure 9. Scan line to determine standardized roughness parameters along the y-axis direction.

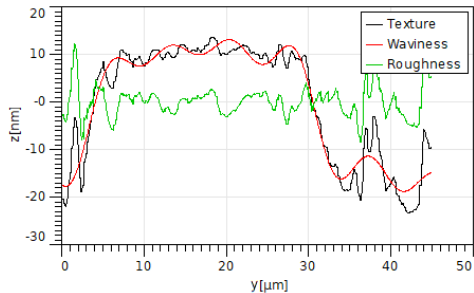


Figure 10. Roughness, texture, and waviness profile along a y-directional scan line as shown in Figure 9.

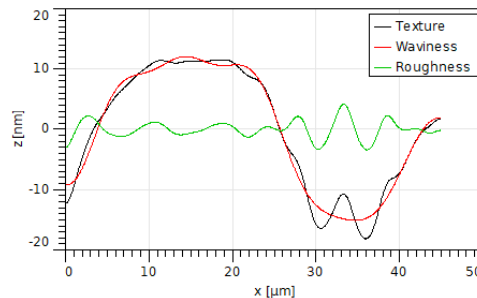


Figure 14. Roughness, texture, and waviness profile along the x-directional scan as shown in Figure 13 after applying a Gaussian filter.

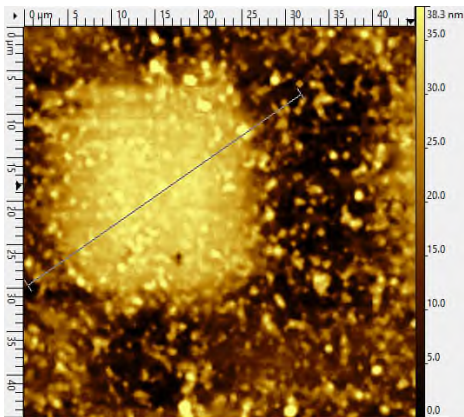
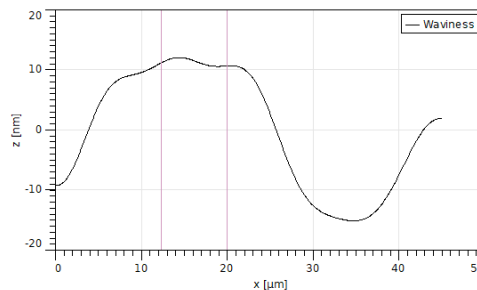


Figure 11. Scan line to determine standardized roughness parameters along an arbitrary diagonal direction.



Points	X [μm]	Y [nm]	Length [μm]	Height [nm]	Angle [deg]
1	12.32	11.18			
2	19.98	10.67	7.66	-0.51	-0.00

Figure 15. Waviness profile measurement over a length on filtered data.

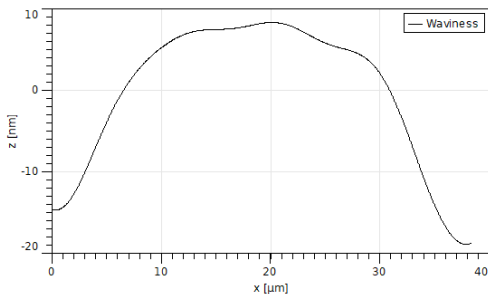
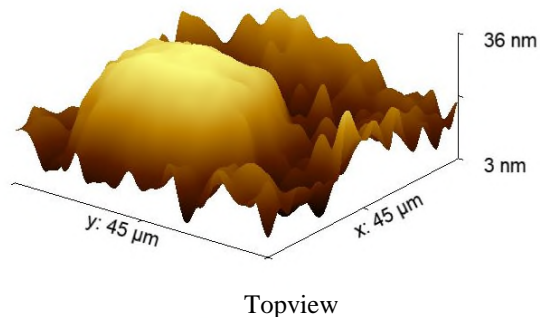
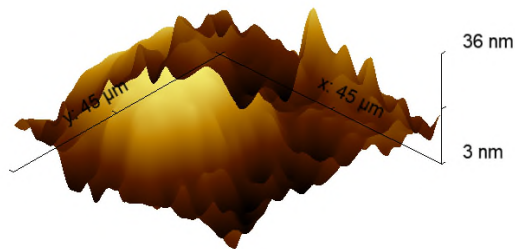


Figure 12. Waviness profile along an arbitrary diagonal direction as shown in Figure 11.



Topview



Bottom view

Figure 16. 3D top and bottom views of the deflection profile after Gaussian filtering.

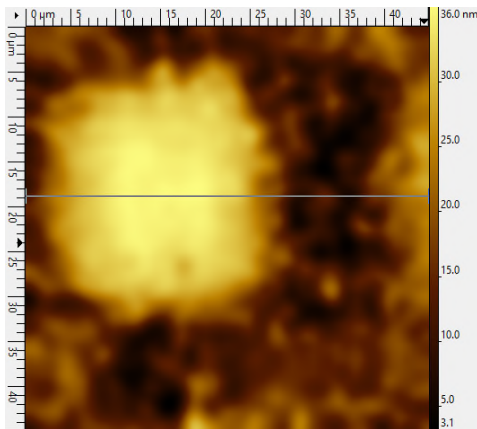


Figure 13. Pseudo-color image of the surface after applying a Gaussian filter.

Figures 7-12 show that using an AFM it is extremely convenient to measure the CMUT diaphragm deflection profile with a very high degree of precision along any direction from which physical properties such as stiffness,

residual stress, etc. of the diaphragm laminate can be extracted using appropriate mathematical models.

Further processing of the AFM data using a Gaussian filter removes the high frequency roughness artifacts further and provides a smoothed out deflection shape of the CMUT diaphragm along an x directional scan line as shown in Figure 13. A 40 pixel magnitude Gaussian filter was used.

The smoothed texture, roughness, and waviness profiles are provided in Figure 14 for comparison. Corresponding waviness values over a length of 7.66 micrometers (two red markers) are shown in Figure 15. The waviness average height (W_a) for this scanned profile is 8.85 nm and maximum height is 11.18 nm to 10.67 nm over this range shows almost a flat surface. Corresponding top and bottom view of the 3D deflection profile are shown in Figure 16.

V. CONCLUSIONS

The presented dynamic mode AFM measurement and data analysis of a CMUT diaphragm appears to be a valuable method to evaluate the deflection profile of a CMUT diaphragm with a very high degree of precision. Main advantage of the proposed method is that the height data is measured directly with nanometer scale precision instead of inferring from a 2D projection of an optical image. Such deflection profiles can be used to determine the residual stress and other physical parameters of a CMUT diaphragm to aid in fine tuning of the process parameters to optimize CMUT diaphragm vibrational characteristics to obtain high quality images. Additionally, the dynamic mode enables to measure the deflection shape of insulating materials, thus enabling to measure the diaphragm shapes where the diaphragm has an insulating top surface. Overall, the dynamic mode AFM can provide high accuracy high resolution nanometer scale measurements to characterize CMUT surfaces.

ACKNOWLEDGMENT

This research work was supported by the Natural Science and Engineering Research Council of Canada (NSERC)'s discovery grant number RGPIN 293218. The authors also greatly acknowledge the generous measurement support provided by Nanosurf™. The authors also acknowledge the collaborative research support provided by the IntelliSense Corporation, Lynnfield, MA, Remcom, PA, Angstrom Engineering, ON, and the CMC Microsystems, Canada.

REFERENCES

[1] A. Ergun, G. Yaralioglu; and B. T. Khuri-Yakub, "Capacitive Micromachined Ultrasonic Transducers: Theory and Technology," *Journal of Aerospace Engineering*, vol. 16, no. 2, pp. 76-84, Apr. 2003,

[2] B. T. Khuri-Yakub and Ö. Oralkan, "Capacitive Micromachined Ultrasonic Transducers for Medical Imaging and Therapy," *Journal of Micromech. and Microeng.*, vol. 21, no. 5, pp. 054004-054014, May, 2011.

[3] M. Klemm, "Acoustic Simulation and Characterization of Capacitive Micromachined Ultrasonic Transducers," Ph.D. dissertation, Dresden University of Technology, TUD Press, Dresden, Germany, 2017.

[4] S. Berg, "Capacitive Micromachined Ultrasonic Transducers," Ph.D. Dissertation, Dept. of Electronics and Telecommunications, Norwegian University of Science and Technology, Trondheim, Norway, 2012.

[5] E. Cianci, et al., "Fabrication Techniques in Micromachined Capacitive Ultrasonic Transducers and their Applications," in MEMS/NEMS Handbook, Springer, Boston, MA, C. Leondes (eds), 2006, pp. 353-382.

[6] S. Savoia, G. Caliano, and M. Pappalardo, "A CMUT Probe for Medical Ultrasonography: From Microfabrication to System Integration," *IEEE Transactions on Ultrasonics, Ferroelectrics, and Frequency Control*, vol. 59, no. 6, pp. 1127-1138, Jun.2012.

[7] A. Unamuno, "New Applications for Ultrasound Technology Through CMUTs," Fraunhofer IPMS, Presentations at the joint event MNBS 2013 and EPoSS general assembly annual forum 2013/epoSS annual-forum-2013-26-september-2013, [Online]. Available from: <http://www.smart-systems-integration.org> Accessed on: Oct. 5, 2020.

[8] M. Rahman, J. Hernandez, and S. Chowdhury, "An Improved Analytical Method to Design CMUTs with Square Diaphragms," *IEEE Transactions on Ultrasonics, Ferroelectrics, and Frequency Control*, vol. 60, no. 4, pp. 834-845, Apr. 2013.

[9] A. Bakhtazad and S. Chowdhury, "An evaluation of optical profilometry techniques for CMUT characterization," *Microsystem Technologies*, Springer, vol. 25, pp. 3627-3642, Sep. 2019.

[10] Nanosurf AG, Switzerland, "Flex-Axiom The most flexible AFM for materials research," [Online]. Available from: <https://www.nanosurf.com/downloads/Nanosurf-Flex-Axiom-Brochure.pdf>, Accessed on: Oct 2, 2020.

[11] L. Charette, N. Cheng, and B. Stuart, "Atomic Force Microscopy," University of British Columbia, [Online]. Available from: <https://phas.ubc.ca/~berciu/TEACHING/PHYS502/PROJECTS/AFM16.pdf>, Accessed on: Oct 2, 2020.

[12] A. Bakhtazad, R. Manwar, and S. Chowdhury, "Fabrication and Characterization of Sealed Cavities Realized by Adhesive Wafer Bonding with Dry Etched Cyclotene," *Microsystem Technologies*, Springer, vol. 21, issue 11, pp. 1-8, Jan. 2015.

[13] Biomedical Engineering Reference In-Depth Information, "Atomic Force Microscopy," [Online]. Available from: <http://what-when-how.com/Tutorial/topic-55ijja/Atomic-Force-Microscopy-10.html>, Accessed on: Sep. 4, 2020.

[14] Park Systems, "How AFM Works," [Online]. Available from: <https://parksystems.com/medias/nano-academy/how-afm-works>, Accessed on: Oct. 4, 2020.

[15] C. Serra-Rodríguez, Re: Can we compare average roughness values obtained from AFM and Optical Profilometer? [Online]. Available from: https://www.researchgate.net/post/Can_we_compare_average_roughness_values_obtained_from_AFM_and_Optical_Profilometer2/52d6cd50d2fd64580c8b45c3/citation/download. 2014, Accessed on: Sep. 10, 2020.

[16] M. Raposo, Q. Ferreira, and P. Ribeiro, "A Guide for Atomic Force Microscopy Analysis of Soft-Condensed Matter", *Modern Research and Educational Topics in Microscopy*, vol. 1, pp. 758-769, Jan. 2007.

[17] Nanosurf AG, Switzerland, Nanosurf FlexAFM Operating Instructions for SPM Control Software, Version 3.1, July 2012. [Online]. Available from: http://www.uel.br/proppg/portalnovo/pages/arquivos/arquivos_gerais/espec/Nanosurf%20FlexAFM%20Operatin%20Instructions.pdf, Accessed on: Sep. 5, 2020.

[18] P. Klapetek, D. Nečas, and C. Anderson, "Gwyddion user guide," [Online]. Available from: <http://gwyddion.net/documentation/user-guide-en/>, Accessed on: Sep. 4, 2020.